Can J Diabetes 43 (2019) 82–89

Contents lists available at ScienceDirect

Canadian Journal of Diabetes

journal homepage: www.canadianjournalofdiabetes.com

Original Research

In Vivo Type 2 Diabetes and Wound-Healing Effects of Antioxidant Gold Nanoparticles Synthesized Using the Insulin Plant *Chamaecostus cuspidatus* in Albino Rats

MohamedIbrahim Ponnanikajamideen PhD [a]; Shanmugam Rajeshkumar PhD [b,*]; Mahendran Vanaja PhD [a]; Gurusamy Annadurai PhD [a]

[a] *Environmental Nanotechnology Division, Sri Paramakalyani Centre for Environmental Sciences Manonmaniam Sundaranar University, Alwarkurichi, Tamilnadu, India*
[b] *Department of Pharmacology, Saveetha Dental College and Hospitals, SIMATS, Chennai, Tamilnadu, India*

Key Messages

- The preparation of antioxidant gold nanoparticles uses the insulin plant *Chamaecostus cuspidatus.*
- The free-radical scavenging properties and antidiabetes activities of antioxidant gold nanoparticles were analyzed.
- The in vivo wound-healing efficacy of antioxidant gold nanoparticles in mice was analyzed.

ARTICLE INFO

Article history:
Received 2 August 2017
Accepted 25 May 2018

Keywords:
antidiabetes
Chamaecostus cuspidatus
gold nanoparticles
wound healing

ABSTRACT

Background: Gold nanoparticles are known for their many applications in the fields of therapeutics and diagnosis.
Methods: This article focuses mainly on the green method of synthesizing gold nanoparticles by using the leaf powder extract of the insulin plant *Chamaecostus cuspidatus* and on the characterization of developed plant-mediated synthesis of gold nanoparticles. Furthermore, we investigated the free-radical scavenging activity of green-synthesized gold nanoparticles.
Results: The free radicals were exhibited in a dose-dependent manner. The 50% inhibition of free radicals by gold nanoparticles showed that it was similar to that of the standard inhibition. Toxicity studies generally examine changes in blood serum chemistry and cell populations in tissue morphology through histologic analysis without inducing any lethal effects in the mouse model, thereby accomplishing sustained control over the progression of diabetes mellitus, which plays a leading role in vascular complications in patients. The treatment by gold nanoparticles of the mice with diabetes for a period of 21 days restored their blood glucose, glycogen and insulin levels.
Conclusions: The use of gold nanoparticles as antidiabetes materials has been achieved. Further studies are required before gold nanoparticle–based drugs are more widely used.

Mots clés :
antidiabétique
Chamaecostus cuspidatus
nanoparticules d'or
guérison d'une plaie

RÉSUMÉ

Contexte : Les nanoparticules d'or sont connues pour leurs nombreuses applications dans les domaines de la thérapeutique et du diagnostic.
Méthodes : Le présent article porte principalement sur la méthode de synthèse verte des nanoparticules d'or à partir de la poudre d'extrait de feuilles de la plante d'insuline *Chamaecostus cuspidatus* et sur la caractérisation de la synthèse médiée par la plante des nanoparticules d'or. De plus, nous avons examiné l'activité de piégeage des radicaux libres des nanoparticules d'or synthétisées par la méthode verte.
Résultats : Les radicaux libres ont été exposés de façon proportionnelle à la dose. L'inhibition de 50 % des radicaux libres par les nanoparticules d'or a montré un résultat similaire avec l'inhibition habituelle. Les études sur la toxicité visent généralement à examiner les modifications de la chimie du sérum sanguin et les populations cellulaires dans la morphologie tissulaire par l'étude histologique sans réduire les effets

* Address for correspondence: Shanmugam Rajeshkumar, PhD, Department of Pharmacology, Saveetha Dental College and Hospitals, SIMATS, Chennai, Tamilnadu 600077, India.
E-mail address: ssrajeshkumar@hotmail.com

1499-2671 © 2018 Canadian Diabetes Association.
The Canadian Diabetes Association is the registered owner of the name Diabetes Canada.
https://doi.org/10.1016/j.jcjd.2018.05.006

létaux dans le modèle de souris, mais pour maîtriser de manière prolongée l'évolution du diabète sucré, qui joue un rôle prépondérant dans la survenue des complications vasculaires chez les patients. Le traitement des souris diabétiques par nanoparticules d'or durant 21 jours rétablit leurs concentrations de glucose dans le sang, en glycogène et d'insuline.
Conclusions : L'utilisation des nanoparticules d'or comme matériaux antidiabétiques a été démontrée; les médicaments à base de nanoparticules d'or seront davantage utilisés s'ils font l'objet d'autres études.

Introduction

In the past 5 decades, nanomedicine has received attention from major world scientists. In the research field as well as on the industrial level, researchers have been working on the improvement of 1- to 100-nm sized nanomaterials. Nanomedicine research is 1 of the upcoming fields in nanotechnology (1–5). Among these fields, the preparation of various nanomaterials has received major consideration because of their distinctive applications in a number of areas (6–10). The occurrence of diabetes has grown worldwide, and it causes serious challenges to public health (11,12), particularly in the form of budget concerns. Diabetes is a severe metabolic disease, and it has been considered one of the world's most deadly diseases. It was reported that by the year 2030, 552 million people may be affected by it (13,14). Diabetes is a chronic disease in which the characteristic element is blood glucose concentrations resulting in a loss of insulin-producing pancreatic beta cells (type 1 diabetes) and a loss of insulin responsiveness in its targets, such as adipose and muscle tissues (type 2 diabetes) (15). Most patients have type 2 diabetes. Nanoparticles are able to act as nanoplatforms for efficient and targeted delivery of drugs and imaging labels by overcoming many biologic and biomedical barriers (16,17). The interesting possible applications of metal nanoparticles are determined by their chemical compositions, sizes, shapes and controlled dispersities (18). Gold nanoparticles are specifically most significant for their exceptional and surface tuneable plasmon resonance (19). Over the past years, the unique colors and typical electronic properties of gold nanoparticles have been improved in biomedical applications (20). Gold nanoparticles are biocompatible and, depending upon the concentration, the gold nanoparticles could also be toxic, which has been proven by in vitro and in vivo approaches (21). The synthesis of metal nanoparticles using plant extract has been a focus in recent years because it is simple and is being a substitute for chemical and physical methods. Gold nanoparticle synthesis using plant extracts has already been reported in the use of various plants, such as *Lippia citriodora*, *Salvia officinalis*, *Pelargonium graveolens* and *Punica granatum*. A lot of consideration has been given to this field because of the variety of plants and their strong potentials to produce nanoparticles with a variety of shapes (22). Against this background, the method of processing the gold nanoparticles as antidiabetes nanomaterials by synthesizing them with pharmacologically key plant materials has been conceived. Many plants with antidiabetes characteristics have been subjected to the synthesis of gold nanoparticles. In this context, the plant *Chamaecostus cuspidatus* has been used to synthesize gold nanoparticles as antidiabetes nanomaterials.

In India, it is known as the insulin plant; it has large fleshy leaves whose undersides are large and smooth and whose dark-green leaves have a light purple shade (23). In our present investigation, the treatment by gold nanoparticles of the mice with diabetes for a period of 21 days restored their blood glucose, glycogen and insulin levels. The use of gold nanoparticles as antidiabetes nanomaterials has been proven, and the gold nanoparticle-based drugs will be more likely to be used if subjected to further studies.

Methods

Chemicals and plant materials

C. cuspidatus leaves were collected from the horticulture department located in Courtallam, Tirunelveli, Tamilnadu, India. The leaves of *C. cuspidatus* were washed with Tween 20 for surface sterilization and washed thoroughly by double-distilled water 3 times. The clean plant leaves were dried in a shady place for a week. The dried leaves were ground into a fine powder; then, 1 g of leaf powder was mixed with 100 mL of distilled water in an Erlenmeyer flask and boiled at 80°C for 20 min. The boiled extract was filtered through Whatman no. 1 filter paper. The collected supernatant was stored at 4°C in the refrigerator for further studies. The analytic-grade chemicals and reagents used in this study were purchased from Sigma Aldrich (Mumbai, India).

Green synthesis of gold nanoparticles

Analytic-grade salt of chloroauric acid tetrahydrate ($HAucl_4$) was used to synthesize gold nanoparticles. For gold nanoparticle synthesis, 10 mL of plant powder extract was added to 1 mM of $HAucl_4$. The mixtures were kept at room temperature on an orbital shaker. The solutions were monitored for gold nanoparticle synthesis at differing time intervals. The synthesized nanoparticles were collected by centrifugation and were used for characterization.

Characterization

The reduction of gold ions into gold nanoparticles was monitored by a double-beam ultraviolet-visible spectrophotometer (Lambda 25; PerkinElmer, Singapore) with a wavelength ranging from 450 to 700 nm. The heat-dried gold nanoparticles were analyzed by x-ray powder diffraction (XRD) (Malvern Panalytical X Pert Powder X celerator diffractometer; Westborough, Massachusetts, United States). The crystalline nature of the nanoparticles was analyzed at the 2 theta range of 20° to 80°. The morphologies and sizes of the gold nanoparticles were found by using a scanning electron microscope (SEM) (PerkinElmer).

The transmission electron microscopy (TEM) method was employed to predict the sizes and shapes of the synthesized gold nanoparticles (CM 200; Philips, Amsterdam, The Netherlands). Thermogravimetric analysis is a method of thermal analysis that is used to analyze the changes in physical and chemical properties of materials. The gold nanoparticles were analyzed at a constant temperature rate and a constant mass by thermogravimetric analysis (Hitachi, Tokyo, Japan).

Free-radical scavenging estimation

α, α-diphenyl-β-picrylhydrazyl radical scavenging activity. The α, α-diphenyl-β-picrylhydrazyl (DPPH) radical-scavenging activity of the gold nanoparticles was determined according to the method followed by Shimada et al (24).

Nitric oxide radical inhibition assay. The inhibition of the nitric oxide radical was assayed according to the method followed by Ebrahimzadeh et al (25).

Superoxide anion-scavenging activity. The superoxide anion-scavenging activity of gold nanoparticles was assayed based on the methods of Nishikimi et al (26).

Lipid peroxidation assay. The lipid peroxidation-scavenging ability of the gold nanoparticles and standards was evaluated using the ammonium thiocyanate method followed by Mitsuda et al (27).

Hydroxyl radical-scavenging activity. The scavenging activity of gold nanoparticles for the hydroxyl radical was carried out using the method of Halliwell and Gutteridge (28).

Reducing power. The reducing power of gold nanoparticles was determined according to the method of Yen and Chen (29).

Acute toxicity studies using gold nanoparticles. In total, 6 mice were used for this study. The mice were randomly divided into 2 groups (n=3 mice per group) as follows: group 1, control; group 2, treated with antioxidant gold nanoparticles.

The mice in group 2 were administered gold nanoparticles suspended in distilled water at a dosage of 1.5 mg/kg body weight (BW)/day, orally, for a period of 10 days. The mice in the control group were treated with double-distilled water alone. At the end of 10 days' treatment, all the mice were starved overnight and sacrificed the next day to determine the toxicity through hematologic and histologic analysis.

Diabetes study. Adult male Wistar mice (150 g to 180 g) were purchased from Venkateshwara Enterprises (Bangalore, India) and maintained at Sri Parama Kalyani Centre for Environmental Sciences (Alwarkurichi, India). Throughout the experiment, the mice were housed in polypropylene cages in an air-conditioned room with a controlled temperature (20°C to 22°C) and automatic lighting (12-h periods of light and dark) and had free access to a standard pellet diet (Pranav Agro, Pune, India) and water. The experiment's protocol was approved by the Animal Ethical Committee of Manonmaniam Sundaranar University, Tirunelveli, India.

Induction of diabetes. Type 2 diabetes was induced by a single intraperitoneal (i.p.) injection of streptozotocin (STZ) (45 mg/kg BW). STZ was freshly dissolved in sodium citrate buffer (pH 4.5, 0.1 M) 15 min after the i.p. administration of nicotinamide (110 mg/kg BW).

Experiment design. In total, 42 mice were divided into 7 groups. Group 1: control rats administered 0.9% saline; group 2: rats administered i.p. STZ 50 mg/kg BW; group 3: rats administered i.p. standard drug (glibenclamide) 50 mg/kg BW; group 4: rats administered i.p. STZ 50 mg/kg BW plus oral administration of 300 mg/kg plant extract of *C. cuspidatus*; group V: rats administered i.p. STZ 50 mg/kg BW plus oral administration of 600 mg/kg plant extract of *C. cuspidatus*; group 6: rats administered i.p. STZ 50 mg/kg BW plus oral administration of 0.75 mg/kg gold nanoparticles synthesized using *C. cuspidatus*; group 7: rats administered i.p. STZ 50 mg/kg BW plus oral administration of 1.5 mg/kg gold nanoparticles synthesized using *C. cuspidatus*.

In vivo wound healing

For this experiment, 12 male Wistar rats (120 g to 160 g) were used. Each in vivo experiment was carried out under in vivo conditions with the permission of the Institutional Animal Ethics Committee of Manonmaniam Sundaranar University, Tirunelveli, India. In brief, the rats were divided into 4 groups, with each group containing 3 rats: group 1, control; group 2, vehicle control H_2O; group 3, treated with green-synthesized gold nanoparticles; group 4, treated with plant extract.

Biochemical analysis. All animals were killed at the end of the experiment; blood was collected, and serum was separated immediately.

Statistical analysis. Statistical analyses were performed using Origin 8.1 software (originLab, Wellesley Hills, Massachusetts, United States). The values are expressed as mean ± SD.

Results and Discussion

The present study was conducted to investigate the antihyperglycemic and antioxidative activities of the leaf extract of *C. cuspidatus* in male albino rats with STZ-induced diabetes. The use of nanomaterials for biomedical applications is a significantly developing branch of nanoscience, so the synthesis of biocompatible nanomaterials using less toxic and more environmentally friendly components is of great importance. In addition, it is significant that the combination of green chemistry principles with nanoscience is 1 of the key issues. New work is being done in nanoparticle synthesis using plant compounds (30–34).

Characterization studies

The ultraviolet-visible spectrophotometry spectra of gold nanoparticles synthesized from *C. cuspidatus* are shown in Supplementary Figure 1. The distinct peak was observed at 462 nm, that is, the surface plasmon resonance of gold nanoparticles, whereas, after the addition of *C. cuspidatus* plant extract, the color of $HAuCl_4$ changed from light yellow to deep blue, which indicates the synthesis of gold nanoparticles in the aqueous solution.

X-ray diffraction analysis

The reduced metal nanoparticles were confirmed as elemental gold using XRD. This analysis was performed to identify the crystalline nature, size and structure of the gold nanoparticles. Supplementary Figure 2 shows the XRD patterns of synthesized gold nanoparticles. The diffraction peak of plant extract-mediated synthesis of gold nanoparticles observed at the 2 theta values of 38°, 44°, 64° and 77° corresponded to the set of lattice planes: (111), (200), (220) and (311), respectively. The peak of synthesized gold nanoparticles was compared with the standard pure gold, which was published by the Joint Committee for Powder Diffraction Set (file 04–0784). The results show that no other peaks were observed in the XRD spectrum; this indicates that the synthesized gold nanoparticles are pure. The inset shows peak broadening of the highest intensity peak parallel to the (111) plane, indicating a reduction in crystallite size. Similar results were reported earlier for gold nanoparticles (35). However, in the present study, the observation of strong peaks indicated that the synthesized gold nanoparticles were pure and crystalline in nature.

SEM analysis

The morphology of the synthesized gold nanoparticles was examined by SEM. The shape and distribution of the gold nanoparticles synthesized by leaf extract of *C. Cuspidatus* are displayed in Supplementary Figure 3. The SEM micrograph clearly indicates that the synthesized nanoparticles were adsorbed on the surface of the plant extract powder. The SEM micrographs showed the synthesized gold nanoparticles in various shapes; most of them are cubic

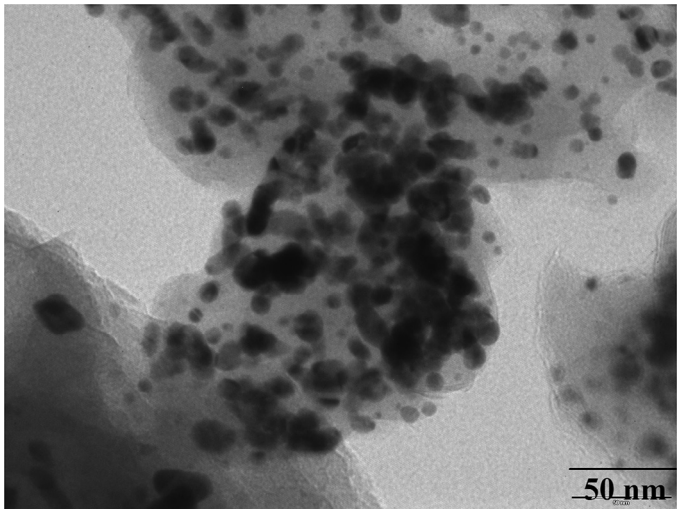

Figure 1. Transmission electron microscopy image of gold nanoparticles synthesized using *Chamaecostus cuspidatus* plant leaf extract.

in nature, with a few occasionally having square-shaped nanoparticles with a size of 2 µm. These results were shown to be in good agreement with earlier reports of biologic nanoparticle synthesis using lemon grass (36). Similar results were observed in the synthesis of gold nanoparticles using *Cassia fistula*. The SEM images exhibited the differing shapes of gold nanoparticles obtained from the bark extract of *C. fistula* (37).

Energy-dispersive x-ray spectroscopy analysis

The energy-dispersive x-ray (EDX) spectra of *C. cuspidatus*-synthesized gold nanoparticles are shown in Supplementary Figure 4. The EDX shows a strong profile at 2 keV, which reveals the presence of gold nanoparticles, whereas the other signals, such as those of oxygen, indicate the accumulation of plant biomolecule extracts with gold nanoparticles. The biomolecules of plant extract play an important role in the reduction of the gold ion into gold nanoparticles. It is 1 of the advantages of the green synthesis of metal nanoparticles when compared to other forms of synthesis. EDX quantitative analysis confirmed that the gold content had the highest elementary composition. Some minor peaks were presented, such as O, Cl, Na, K and Fe, but these compounds are derived from plant biomolecules. Similar results were reported in the synthesis of gold nanoparticles using plant extract of *Mentha piperita*. The results suggested that the gold nanoparticles are synthesized due to the action of the plant extract, which acts as a good reductant for biosynthesis (38).

TEM analysis

The morphologies and sizes of nanoparticles in green-synthesized gold nanoparticles were determined through TEM images (Figure 1). The *C. cuspidatus*-synthesized gold nanoparticles were monodispersed and mostly spherical in shape, with an average size of 50 nm. The spherical and undefined shapes, also found in the TEM images, showed that these particles are synthesized at the beginning of the reaction, i.e. at 10 min to 2 h of incubation. After 2 h of incubation, the particles were aggregated and formed a bulk structure. The low absorbance was observed after 2 h in the ultraviolet-visible spectrophotometry spectrum, which also proved the aggregation of particles. The gold nanoparticles synthesized from a plant extract of *Murray koenigii* (39) matched with our present report. Similar results suggest that in the synthesis of gold nanoparticles with the plant extract *Cassia auriculata*, the particles formed were spherical, hexagonal and triangular in shape (40).

Thermogravimetric analysis

Thermogravimetric analysis showed that upon heating the mass of the sample initially, the rates of mass slowly decreased but then gradually increased. The total mass loss was 35.0%, which was assigned to loose gold metal (Supplementary Figure 5). Corresponding to the initial slow mass loss was an exothermic region in the differential calorimetric data. In the case of the total green-synthesized gold nanoparticles, weight loss occurred between 240°C and 360°C, relating to the thermal degradation of the gold nanoparticles. The gold nanoparticles showed a 1% weight loss up to 102°C, and this could be due to the loss of the external water molecule. Furthermore, a slow weight loss of about 3.0% between 102°C and 360°C was due to the slight decomposition of the materials (41). Similar reports were observed in the work of Fan et al (42), which demonstrated that the integrity of amino acids in maintaining high coupling activity could be achieved by the coating of gold nanoparticles.

Antioxidant study

DPPH radical activity. The proportion of plant extract in the DPPH-free radicals via hydrogen-donating activity was 96.63%, and the gold nanoparticles in the DPPH-free radical activity was 97.05%; for standard vitamin C, it was found to be 91.15%, as shown in Figure 2. DPPH scavenging was increased in a concentration-dependent manner compared to ascorbic acid and was used as the positive antioxidant control in this investigation. The inhibitor concentration that decreases the biotransformation of a substrate at a single, specified concentration by 50% (IC_{50}) of the value of a plant extract is 43.48 µg/mL, and that of the gold nanoparticles is 48.96 µg/mL. A similar report by Mubarak et al (38) showed that DPPH scavenging was increased in a concentration-dependent manner compared to that of ascorbic acid; it was used as the positive antioxidant control in that investigation.

Nitric oxide assay. The green-synthesized gold nanoparticles increased nitric oxide radical-scavenging activity above that of the plant-leaf powder. The radical-scavenging activity increased when the concentration of gold nanoparticles was increased. When compared to the nitric oxide radical-scavenging activity of raw plant extract, the green-synthesized gold nanoparticle activity was slightly increased in a dose-dependent manner (Supplementary Figure 6). The IC_{50} value of the gold nanoparticles was 45.65 µg/mL and for the plant, the extract was 49.33 µg/mL. These results show that gold nanoparticles are an excellent antioxidant agent.

Superoxide anion activity. The results of the superoxide anion-scavenging activity of gold nanoparticles and raw plant extract are shown in Supplementary Figure 7. The decreased absorbance at 560 nm with the gold nanoparticles indicates the consumption of superoxide anions in the reaction mixture. The gold nanoparticles showed the scavenging activity; the IC_{50} value was 46.84 µg/mL, and the plant extract IC_{50} value was 45.01 µg/mL (Supplementary Figure 7). Similar results were reported by Babu et al (43). Triphala, an Ayurvedic herbal rasayana formula extract, shows that superoxide scavenging activity is due to the presence of phenolic compounds.

Lipid peroxidation assay. The lipid peroxidation inhibition assay was conducted using the raw plant extract and gold nanoparticles, which were compared with standard vitamin E. The gold nanoparticles had strong inhibition activity when compared to the raw plant extract in controlling lipid peroxidation. The scavenging activity increased

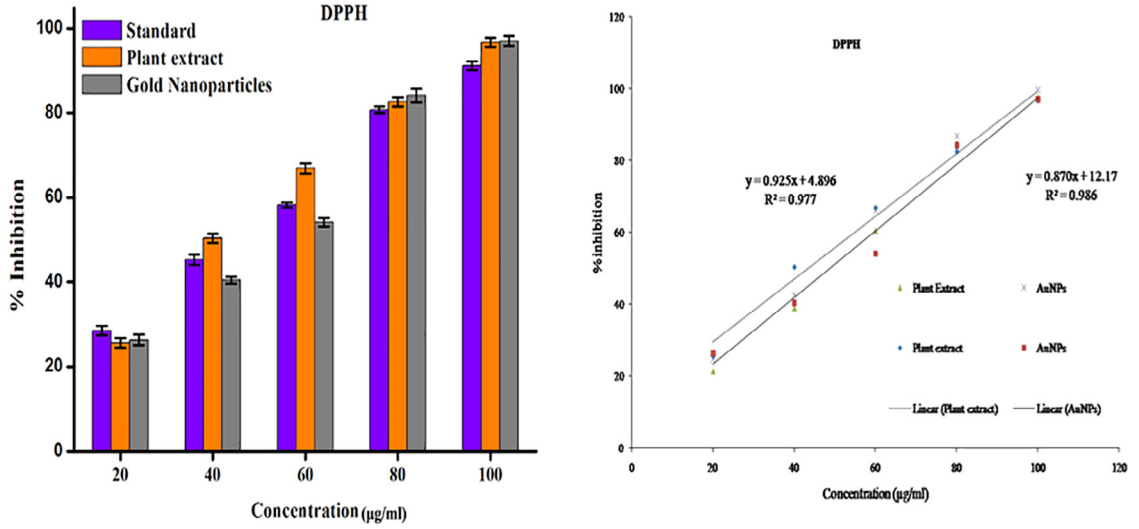

Figure 2. 2,2-diphenyl-1-picrylhydrazyl (DPPH) radical scavenging effect of gold nanoparticles and *Chamaecostus cuspidatus* plant extract. *AuNPs*, gold nanoparticles.

when the concentrations of gold nanoparticles and the raw plant extract were raised. The IC_{50} value of the gold nanoparticles was 48.31 µg/mL, and that of the plant extract was 52.51 µg/mL (Supplementary Figure 8).

Hydroxyl radical assay. The scavenging activity of the raw plant extract was 87.33%, and that of the gold nanoparticles was 92.95%, respectively (Supplementary Figure 9). The IC_{50} value of gold nanoparticles was 47.06 µg/mL, and that of the plant extract was 50.71 µg/mL. The activity was more effective in quenching the hydroxyl radicals produced in the reaction mixture. The hydroxyl radical can induce oxidative damage to DNA, lipids and proteins (44).

Reducing power. The reducing power of both plant extract and gold nanoparticles increased with increases in concentration. The gold nanoparticles showed more effective reducing ability when compared to raw plant extract (Supplementary Figure 10). In this assay, Fe(III) reduction is often used as a significant indicator of electron-donating activity, which is an important mechanism of phenolic antioxidant action (45). This is correlated with the presence of reductones, which exhibit their antioxidant action by breaking the radical chain and donating a hydrogen atom (46). The gold nanoparticles showed the highest activity in a dose-dependent manner due to the presence of more reductones in the higher doses.

In vivo toxicity studies. In this study, the mice were orally injected with gold nanoparticles at a dosage of 1.5 mg/kg BW/day for 10 days. We then examined the morphology and behavioural changes once daily. All the mice survived throughout the experiment period without exhibiting any abnormalities. The mice did not show any symptoms of toxicity, such as fatigue, loss of appetite, change in fur colour, weight loss, etc. Comparative analyses of various hematologic parameters in the control animals and those treated with gold nanoparticles clearly showed that there was no significant alteration except marginal variations in certain parameters (Supplementary Table 1). The pathologic effect of nanoparticles on the morphologic characteristics of the organs was examined through histologic observations by using light microscopy. The histologic findings exhibited the nontoxic effect of gold nanoparticles on the liver, kidney and lung (Figure 3). The reports obtained from Dr. Syed Suliman of the Tirunelveli Medical College Hospital (Tirunelveli, India) confirmed that the organs treated with gold nanoparticles did not showed any significant morphologic changes in comparison to the control organs. The histologic sections of lung tissue from the control animals showed regular alveolar geometry and normal alveolar septa (Figure 3A). Similarly, lung tissues

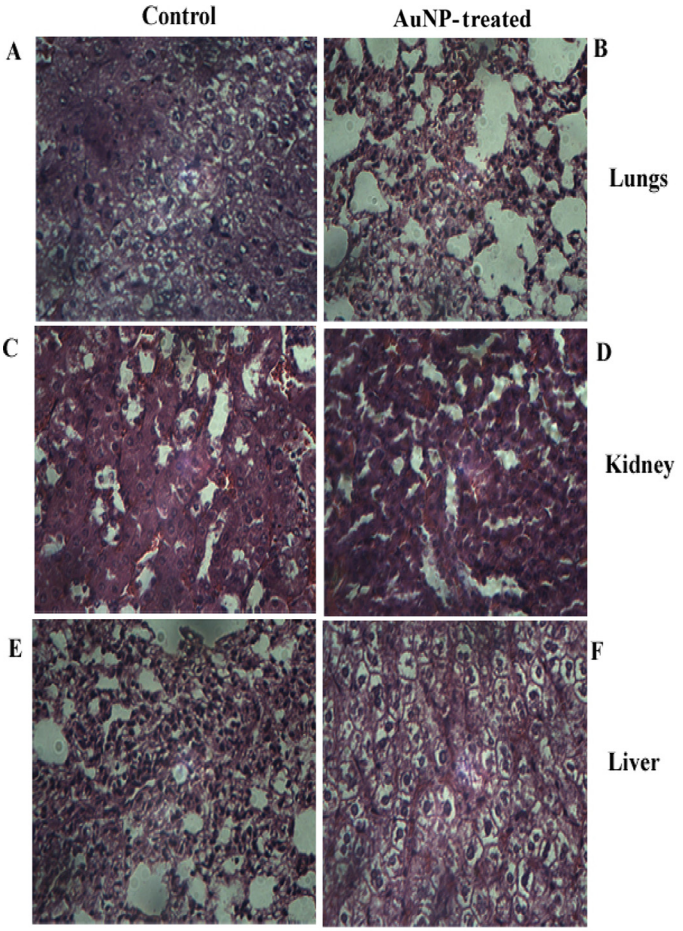

Figure 3. Toxicity studies of gold nanoparticles in mouse organs. *AuNP*, gold nanoparticle.

treated with gold nanoparticles (Figure 3B) showed normal alveolar membranes and common blood vessels. The kidney sections of control animals showed the presence of usual renal cortex and glomerular tufts (Figure 3C), and the histologic sections of animals treated with gold nanoparticles did not show any changes in the kidney tissue. (Figure 3D). The histologic sections of liver from the control animals showed normal hepatic portals and central veins (Figure 3E). The liver treated with gold nanoparticles also showed normal hepatocytes and a clear vein with no morphologic changes when compared to control animals (Figure 3F). These studies clearly confirm the nontoxic nature of biologically synthesized gold nanoparticles in the in vivo system. Cells are capable of taking the gold nanoparticles without any cytotoxic effects (47). The nontoxic effect of the gold nanoparticles was confirmed by the study; no subclinical toxicology was shown in the histologic studies of the vital organs (lung, kidney and liver) after the administration of gold nanoparticles for 10 days. These results correlated with previous reports of using the gold nanoparticles as an antioxidative agent and to control hypoglycemic conditions (48).

In vivo antidiabetes studies: effect on BW. The effect of gold nanoparticles on BW was studied using in vivo animal models. The rats treated with STZ showed significant weight loss, but the rats treated with gold nanoparticles showed normalization of BW and also weight gain due to their growth (Supplementary Figure 11). These data indicate that the increased level of glucose in rats with STZ-induced diabetes was a low level that was achieved by the oral administration of gold nanoparticles synthesized from *C. cuspidatus*. For this experiment, the BW was measured before and after treatment. Before treatment, the rats were at a normal weight; after treatment, significant ($p<0.05$) weight loss occurred. The BW of rats administered *C. cuspidatus* slightly decreased when compared to control rats with diabetes and rats administered standard drugs. The BW of rats treated with gold nanoparticles significantly increased when compared to the control rats (Supplementary Table 2).

Effect on blood glucose, insulin and glycogen. To examine the effect of gold nanoparticles on the levels of blood glucose, insulin and glycogen, the rats were treated with STZ (Supplementary Figure 12). The decrease in glucose levels in group 7 rats with diabetes suggests that the synthesized gold nanoparticles exert insulin-like results on marginal tissues, either by promoting the uptake of glucose or by inhibiting hepatic gluconeogenesis (49). The rats with diabetes in groups 4 and 5, which were administered *C. cuspidatus*, showed slightly increased blood glucose levels, but the insulin and glycogen levels remained balanced. However, among the rats with diabetes in groups 6 and 7, those that were treated with gold nanoparticles showed no changes in blood glucose, insulin or glycogen levels. It was observed that all biochemical values varied slightly when compared to those of normal mice. As a result of extensive screening after various dosages of plant extracts (300 or 600 mg/kg) and gold nanoparticles (0.75 or 1 mg/kg), the rats treated with the gold nanoparticles did not show any significant effects (Supplementary Table 3). However, the metal nanoparticles improved glucose consumption and metabolism through their potent influence on improvement of hepatic glycogenesis through action on the insulin-signaling pathway (50). Similar results showed significant reductions in blood glucose levels in the groups with diabetes that were treated with zinc oxide nanoparticles, single nucleotide polymorphisms or insulin (75.8%, 68.2% and 84.2%, respectively) (51). The therapeutic efficacy of bergenin was examined in mice with type 2 diabetes, and similar findings, reported by Ambika and Saravanan (52), showed improvements in liver tissue, hyperglycemia, insulin sensitivity, glucose uptake and hepatoprotectiveness. Hence, it might be used in the management of obesity-associated type 2 diabetes mellitus.

Effect on serum protein and total cholesterol levels. The serum protein and cholesterol levels showed slight changes in the control rats with diabetes, and the rats treated with gold nanoparticles (0.75, 1 mg/kg) showed levels of serum protein and total cholesterol similar to those of the control mice with diabetes that were administered plant extract (Supplementary Figure 13). The rats treated with plant extract (300 or 600 mg/kg) showed significant ($p<0.05$) changes in cholesterol levels, but the serum protein levels remained unchanged. The results of the present study indicated that the animals showed regulation of the metabolic process and restoration of the cholesterol and serum protein levels to near normal. The induction of diabetes with STZ was associated with a characteristic loss of BW, which was due to increased muscle wasting (53). The present study showed that the gold nanoparticles synthesized using *C. cuspidatus* are very effective in inducing hypoglycemic activity (Supplementary Table 4).

In vivo wound healing. Gold nanoparticles and plant extracts were used for the wound-healing test (Figure 4). At the initial stage (the first week), healing was observed in rats treated with both gold nanoparticles and plant extract when compared to the controls. However, in the fourth week after wounding, it was observed that the rats treated with gold nanoparticles and plant extract showed greater healing responses than did the control rats. In the fourth week after the treatments, the healing percentages of the 4 groups—control, vehicle control H_2O, gold nanoparticle and plant extract-treated wounds—were 78%, 97%, 66% and 64%, respectively. These data indicate that the plant extracts and the gold nanoparticles produced the most significant healing activity ($p<0.01$); the antioxidant and anti-inflammatory properties of green-synthesized gold nanoparticles showed their healing abilities even more profoundly with time. We evaluated the progress of wound healing in differently treated groups and studied the commencement of apoptosis during the course of wound healing. Previous studies have shown that gold nanoparticles have cutaneous wound-healing abilities through their anti-inflammatory and antioxidation effects (54). These findings support the potential role of gold nanoparticles in the treatment of cutaneous wounds (Supplementary Table 5).

Conclusions

Gold nanoparticles are recognized for their wide application in the field of therapeutics and diagnosis. The present study was carried out to study the hypoglycemic effects of the extract of *C. cuspidatus* in healthy rats and rats with STZ-induced diabetes. *C. cuspidatus* is reported to have medicinal and traditional values, including hypoglycemic properties. In the antidiabetes study, the blood, glucose and glycogen levels of the test animals showed that the extract had significant hypoglycemic activity when compared to the control group with diabetes; the effects of various dosages of extract were studied in rats with STZ-induced diabetes and in rats without diabetes. The results also indicated dose-dependent effects. The synthesized gold nanoparticles are nontoxic and have defensive effects on the organs. The cutaneous wound-healing activity of green-synthesized gold nanoparticles showed significantly greater wound recovery when compared to controls, so these findings reveal that further study of wound healing in patients with diabetes is warranted. Moreover, we conclude that the overall results of the experiments have shown that the prospective properties of gold nanoparticles synthesized by plant extracts of *C. cuspidatus* show higher activity with less amount and lower costs than do alternatives for treatment of diabetes. Our study has opened avenues for further research, especially with reference to the development of a potent formulation for use in patients with diabetes mellitus.

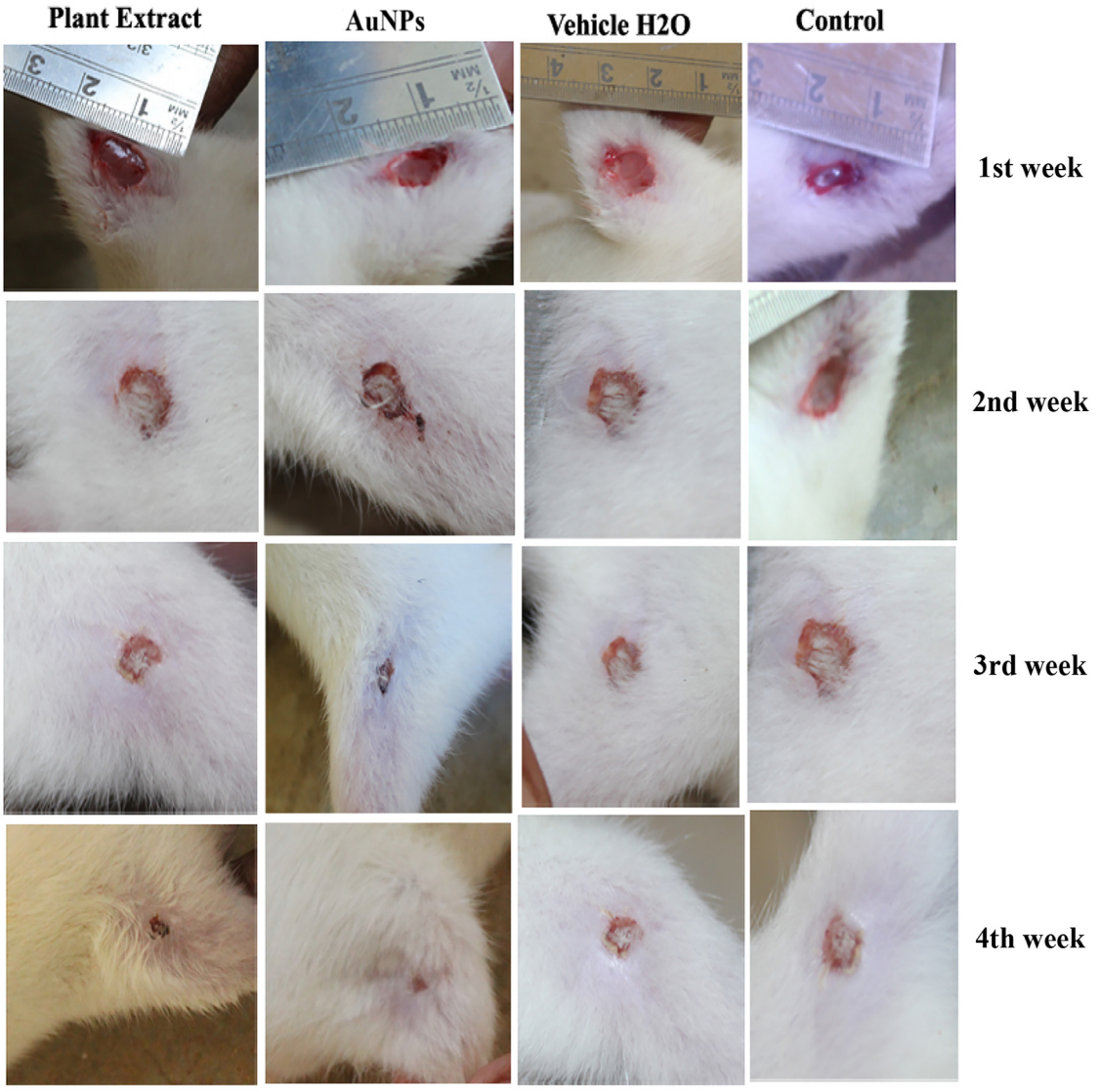

Figure 4. Macroscopic appearance of wound repair with positive control, vehicle H_2O as control, *Chamaecostus cuspidatus* extract and gold nanoparticles at differing postwounding days. *AuNPs*, gold nanoparticles.

Supplementary Material

To access the supplementary material accompanying this article, visit the online version of *Canadian Journal of Diabetes* at https://www.canadianjournalofdiabetes.com.

Acknowledgments

The authors gratefully acknowledge the program sponsored by the Educational Institutions-Department of Science Technology (DST-FIST), New Delhi, India, for funding (S/FST/ESI-101/2010) the research development to carry out this work.

Author Disclosures

Conflicts of interest: None.

Author Contributions

MP carried out antidiabetic activity, MV carried out wound healing activity, SR and GA designed the work and wrote and corrected the manuscript.

References

1. Halperin A. Polymeric micelles: A star model. Macromolecules 1987;20:2943–6.
2. Lammers T. Smart drug delivery systems: back to the future vs. clinical reality. Int J Pharm 2013;454:527–9.
3. Davis ME, Chen Z, Shin DM. Nanoparticle therapeutics: an emerging treatment modality for cancer. Nat Rev Drug Discov 2008;7:771–82.
4. Sengupta S, Kulkarni A. Design principles for clinical efficacy of cancer nanomedicine: A look into the basics. ACS Nano 2013;7:2878–82.
5. Wagner V, Dullaart A, Bock AK, Zweck A. The emerging nanomedicine landscape. Nat Biotechnol 2006;24:1211–7.
6. Zinatloo-Ajabshir S, Salavati-Niasari MJ. Preparation of nanocrystalline cubic ZrO2 with different shapes via a simple precipitation approach. J Mater Sci: Mater Electron 2016;27:3918.

7. Link S, Wang ZL, El-Sayed MA. Alloy formation of gold–silver nanoparticles and the dependence of the plasmon absorption on their composition. J Phys Chem B 1999;103:529.
8. Zinatloo-Ajabshir S, Salavati-Niasari M. A sonochemical-assisted synthesis of pure nanocrystalline tetragonal zirconium dioxide using tetramethylethylenediamine. Int J Appl Ceram Technol 2014;11:654.
9. Yan Y, Sun B, Ma DJ. Resistive switching memory of single $BiMnO_{3+\delta}$ nanorods. J Mater Sci: Mater Electron 2016;27:512.
10. Sun B, Zhao W, Wei L, Li H, Chen P. Enhanced resistive switching effect upon illumination in self-assembled NiWO4 nano-nests. Chem Commun 2014;50:131–42.
11. Yang Y, Xia T, Chen F, et al. Electrospun fibers with plasmid bFGF polyplex loadings promote skin wound healing in diabetic rats. Mol Pharmaceut 2012;9:48–58.
12. Yannas IV, Kwan MD, Longaker MT. Early fetal healing as a model for adult organ regeneration. Tissue Eng 2007;13:1789–98.
13. Venkatachalam M, Govindaraju K, Mohamed Sadiq A, Tamilselvan S, Ganesh Kumar V, Singaravelu G. Functionalization of gold nanoparticles as antidiabetic nanomaterials. Spectrochim Acta A Molec Biomolec Spectrosc 2013;116:331–8.
14. King H, Albert RE, Herman WH. Global burden of diabetes, 1995–2025: prevalence, numerical estimates, and projections. Diabetes Care 1998;21:1414–31.
15. Schwarz PE, Li J, Lindstrom J, Tuomilehto J. Tools for predicting the risk of type 2 diabetes in daily practice. Horm Metab Res 2009;41:86–97.
16. Grodzinski P, Silver M, Molnar LK. Nanotechnology for cancer diagnostics: Promises and challenges. Exp Rev Mol Diagn 2006;6:307–18.
17. Sahoo SK, Parveen S, Panda JJ. The present and future of nanotechnology in human health care. Nanomedicine (Lond) 2007;3:20–31.
18. Tinder P. Determination of blood glucose using an oxidase-peroxidase system with a non-carcinogenic chromogen. Ann Clin Biochem 1969;6:24–9.
19. Burke TR, Ye B, Yan X, et al. Small molecule interactions with protein-tyrosine phosphatase PTP1B and their use in inhibitor design. Biochemistry 1996;35:15989–96.
20. Dreaden EC, Alkilany AM, Huang X, Murphy CJ, El- Sayed MA. The golden age: Gold nanoparticles for biomedicine. Chem Soc Rev 2012;41:2740–79.
21. Jain S, Hirst DG, Brit JM. Gold nanoparticles as novel agents for cancer therapy. J Radiol 2012;85:101–13.
22. Elia P, Zach R, Hazan S, Kolusheva S, Porat Z, Zeiri Y. Green synthesis of gold nanoparticles using plant extracts as reducing agents. Int J Nanomed 2014;9:4007–21.
23. Sheety A. Effect of the insulin plant (Costus igneus) leaves on dexamethasone-induced hyperglycemia. Int J Ayurveda Res 2010;1:100–2.
24. Shimada K, Fujikawa K, Yahara K, Nakamura T. J Agr Food Chem 1992;40:945–8.
25. Ebrahimzadeh MA, Nabavi SM, Nabavi SF, Bahramian F, Bekhradnia AR. Antioxidant and free radical scavenging activity of *H. officinalis L. var. angustifolius, V. odorata, B. hyrcana* and *C. speciosum*. Pak J Pharm Sci 2010;23:29–34.
26. Nishikimi M, Kawai T, Yagi K. Guinea pigs possess a highly mutated gene for L-gulono-gamma-lactone oxidase, the key enzyme for L-ascorbic acid biosynthesis missing in this species. J Biol Chem 1992;267:21967–72.
27. Mitsuda H, Yasumoto K, Iwami K. Antioxidative action of indole compounds during the autoxidation of linoleic acid. Eiyo to Shokuryo 1966;19:210–4.
28. Halliwell B, Gutteridge JMC, Aruoma OI. The deoxyribose method: A simple "test-tube" assay for determination of rate constants for reactions of hydroxyl radicals. Anal Biochem 1987;165:215–24.
29. Yen CY, Chen HY. Antioxidant activity of various tea extracts in relation to their antimutagenicity. J Agri Food Chem 1995;43:27–32.
30. Kasthuri J, Kathiravan K, Rajendiran N. Phyllanthin-assisted biosynthesis of silver and gold nanoparticles: a novel biological approach. J Nanopart Res 2009;11:1075–108.
31. Karthick V, Ganesh Kumar V, Maiyalagan T, et al. Green synthesis of well dispersed nanoparticles using leaf extract of medicinally useful *Adhatoda vasica* Nees. Micro Nanosyst 2012;4:192–8.
32. Khaleel Basha S, Govindaraju K, Manikandan R, Ahn JS, Bae EY, Singaravelu G. Phytochemical mediated gold nanoparticles and their PTP 1B inhibitory activity. Colloids Surf B Biointerf 2010;75:405–9.
33. Govindaraju K, Kiruthiga V, Manikandan R, Ashokkumar T, Singaravelu G. Investigation of h-BN/Rh(111) nanomesh interacting with water and atomic hydrogen. Mater Lett 2011;65:256–9.
34. Ganesh Kumar V, Dinesh Gokavarapu S, Rajeswari A, et al. Facile green synthesis of gold nanoparticles using leaf extract of antidiabetic potent *Cassia auriculata*. Colloids Surf B: Biointerf 2011;87:159–63.
35. Philip D, Unni C, Aswathy Aromal S, Vidhu VK. Murraya Koenigii leaf-assisted rapid green synthesis of silver and gold nanoparticles. Spectrochim Acta A 2011;78:899–904.
36. Shankar SS, Rai A, Ankamwar B, Singh A, Ahmed A, Sastry M. Biological synthesis of triangular gold nanoprisms. Nat Mater 2004;3:482–8.
37. Daisy P, Saipriya K. Biochemical analysis of *Cassia fistula* aqueous extract and phytochemically synthesized gold nanoparticles as hypoglycemic treatment for diabetes mellitus. Int J Nanomed 2012;7:1189–202.
38. Mubarak Ali D, Thajuddin N, Jeganathanb K, Gunasekaran M. Plant extract mediated synthesis of silver and gold nanoparticles and its antibacterial activity against clinically isolated pathogens. Colloid Surf B Biointerf 2011;85:360–5.
40. Ganesh Kumar V, Dinesh Gokavarapu S, Rajeswari A, et al. Facile green synthesis of gold nanoparticles using leaf extract of antidiabetic potent *Cassia auriculata*. Colloid Surf B Biointerfac 2011;87:159–63.
41. Mohammad F, Arfin T. Thermodynamics and electrochemical characterization of core-shell type gold–coated superparamagnetic iron oxide nanoparticles. Adv Mat Lett 2014;6:315–24.
42. Fan J, Chen S, Gao Y. Coating gold nanoparticles with peptide molecules via a peptide elongation approach. Colloid Surf B: Biointerfac 2003;28:199–207.
43. Babu D, Gurumurthy P, Borra SK, Cherian KM. Antioxidant and free radical scavenging activity of triphala determined by using different in vitro models. J Medicin Plant Res 2013;7:2898–905.
44. Spencer JPE, Jenner A, Aruoma OI. Intense oxidative DNA damage promoted by L-DOPA and its metabolites Implications for neurodegenerative disease. FEBS Lett 1994;353:246–50.
45. Nabavi SM, Ebrahimzadeh MA, Nabavi SF, Hamidinia A, Bekhradnia AR. Determination of antioxidant activity, phenol and flavonoid content of *Parrotia persica* Mey. Mey Pharmacologyonline 2008;2:560–7.
46. Gordon MH. The mechanism of antioxidant action in vitro. London, United Kingdom: Elsevier Applied Science 1990, pgs. 1–18.
47. Connor EE, Mwamuka J, Gole A, Murphy CJ, Wyatt MD. Gold nanoparticles are taken up by human cells but do not cause acute cytotoxicity. Small 2005;1:325–7.
48. Kanth SBM, Kalishwaralal K, Sriram M, et al. Anti-oxidant effect of gold nanoparticles restrains hyperglycemic conditions in diabetic mice. J Nanobiotechnol 2010;8:16.
49. Ali L, Azad Khan AK, Mamun MIR, et al. Studies on the hypoglycemic effects of fruits pulp, seed and whole plant of *Momordica charantia* on normal and diabetic model rats. Plant Med 1993;59:408–12.
50. Jansen J, Karges W, Rink L. Zinc and diabetes–clinical links and molecular mechanisms. J Nutr Biochem 2009;20:399–417.
51. Alkaladi A, Abdelazim AM, Mohamed Afifi M. Antidiabetic activity of zinc oxide and silver nanoparticles on streptozotocin-induced diabetic rats. Int J Mol 2014;15:2015–23.
52. Ambika S, Saravanan R. Effect of bergenin on hepatic glucose metabolism and insulin signaling in C57BL/6J mice with high fat-diet induced type 2 diabetes. J Appl Biomed 2016;7:221–7.
53. Swanston-Flat SK, Day C, Bailey CJ, Flatt PR. Traditional plant treatments for diabetes. Studies in normal and streptozotocin diabetic mice. Diabetologia 1990;33:462–4.
54. Leu J-G, Chen S-A, Chen H-M, et al. The effects of gold nanoparticles in wound healing with antioxidant epigallocatechin gallate and α-lipoic acid. Biol Med 2012;8:767–75.

Supplementary Material

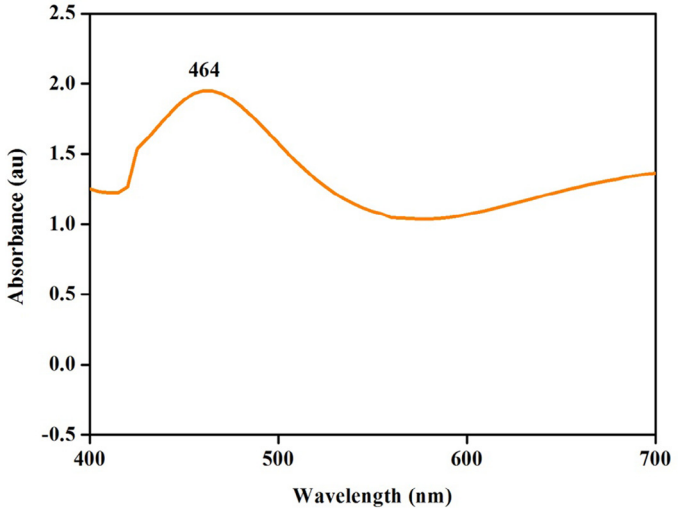

Figure S1. Ultraviolet-visible spectroscopic analysis of gold nanoparticles synthesized using *C. cuspidatus* plant extract. *au*, arbitrary unit.

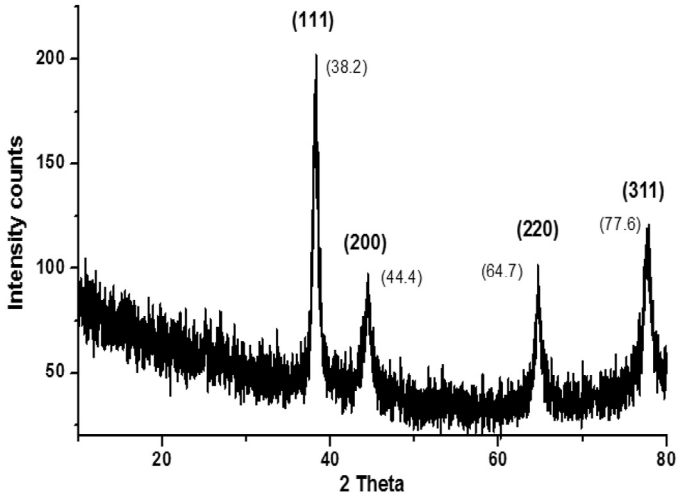

Figure S2. X-ray powder diffraction spectra of gold nanoparticles synthesized using *Chamaecostus cuspidatus* plant extract.

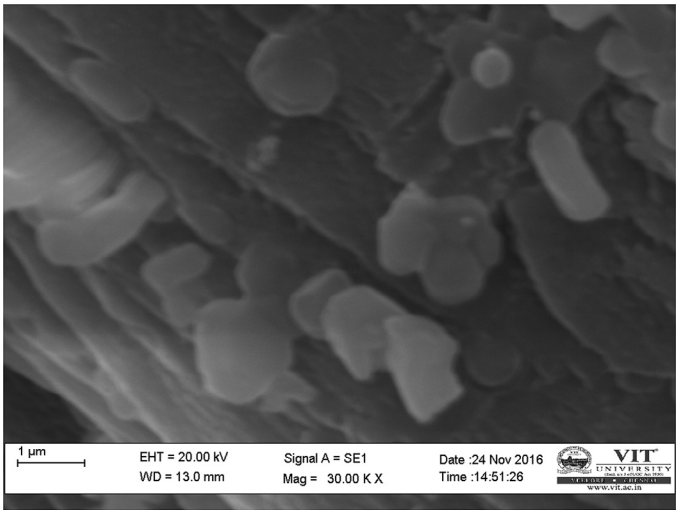

Figure S3. Standard error of the mean images of gold nanoparticles synthesized using *Chamaecostus cuspidatus* plant leaf extract.

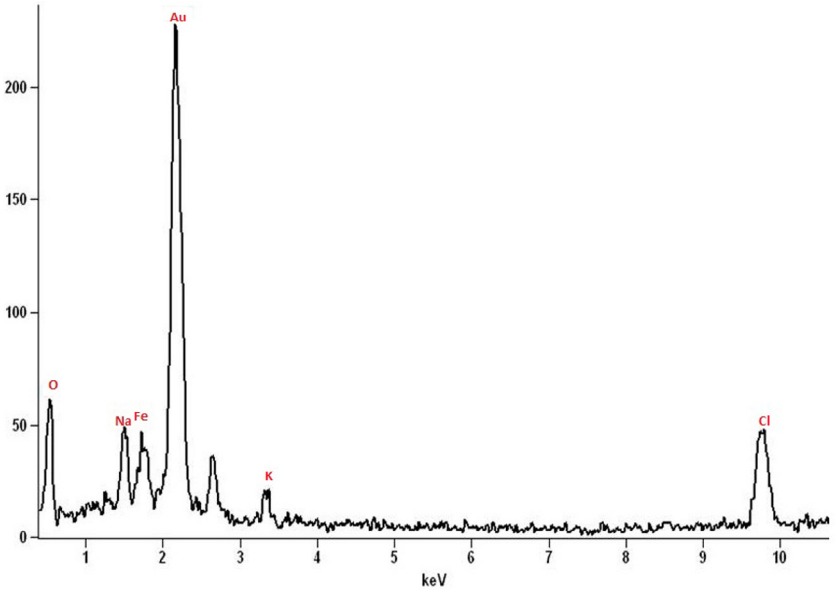

Figure S4. Energy dispersive x-ray spectroscopy spectrum of gold nanoparticles.

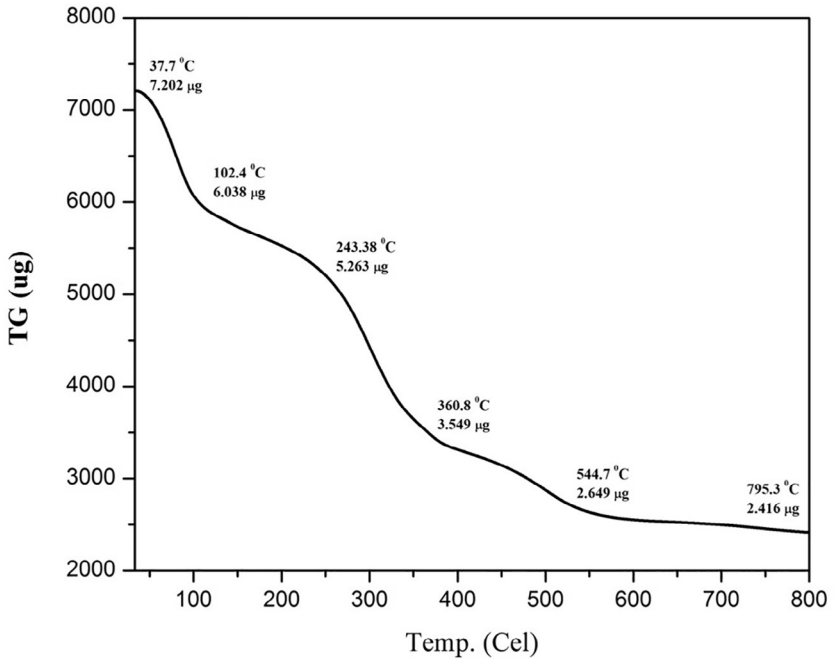

Figure S5. Thermogravimetric (TG) analyses of gold nanoparticles heated at 37°C to 795°C. *Cel*, Celsius.

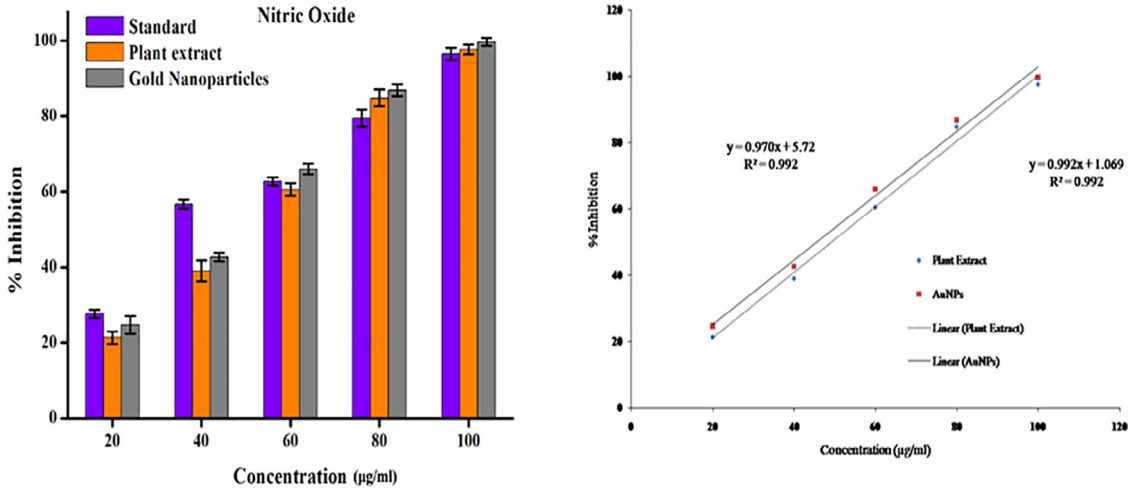

Figure S6. Antioxidant activity of gold nanoparticles and *Chamaecostus cuspidatus* plant extract by nitric oxide inhibition assay. *AuNPs*, gold nanoparticles.

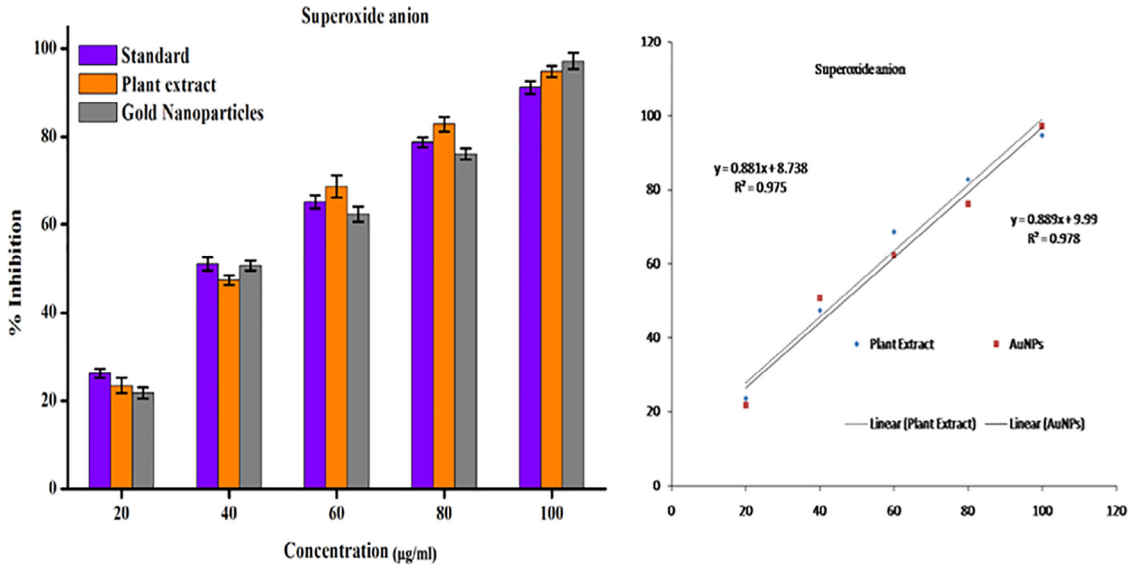

Figure S7. Antioxidant activity of gold nanoparticles and *Chamaecostus cuspidatus* plant extract by superoxide anion scavenging activity. *AuNPs*, gold nanoparticles.

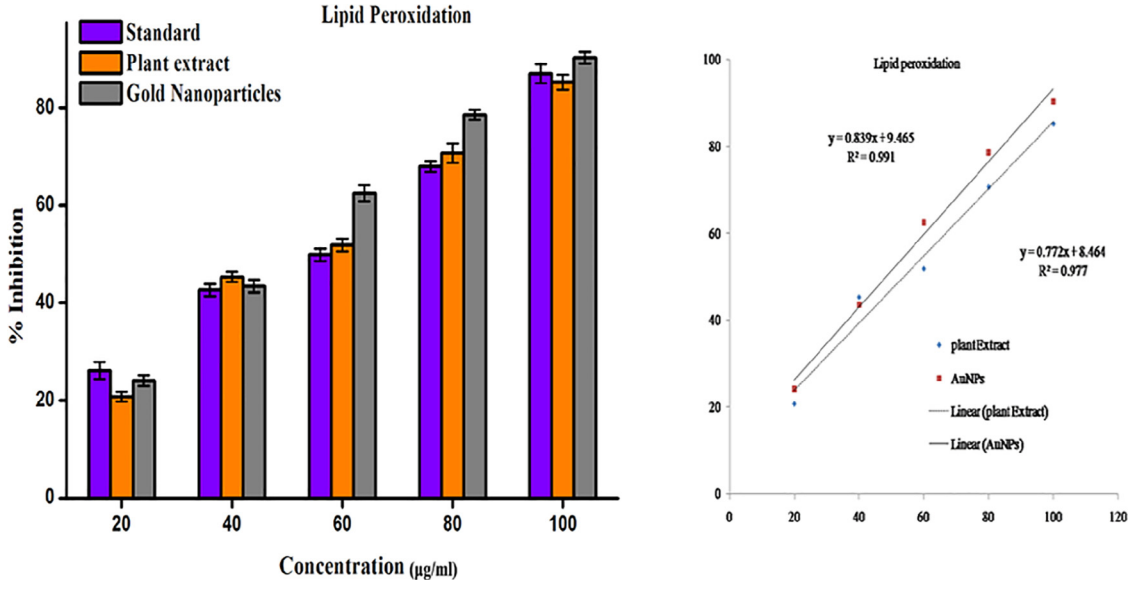

Figure S8. Antioxidant activity of gold nanoparticles and *Chamaecostus cuspidatus* plant extract by lipid peroxidation assay. *AuNPs*, gold nanoparticles.

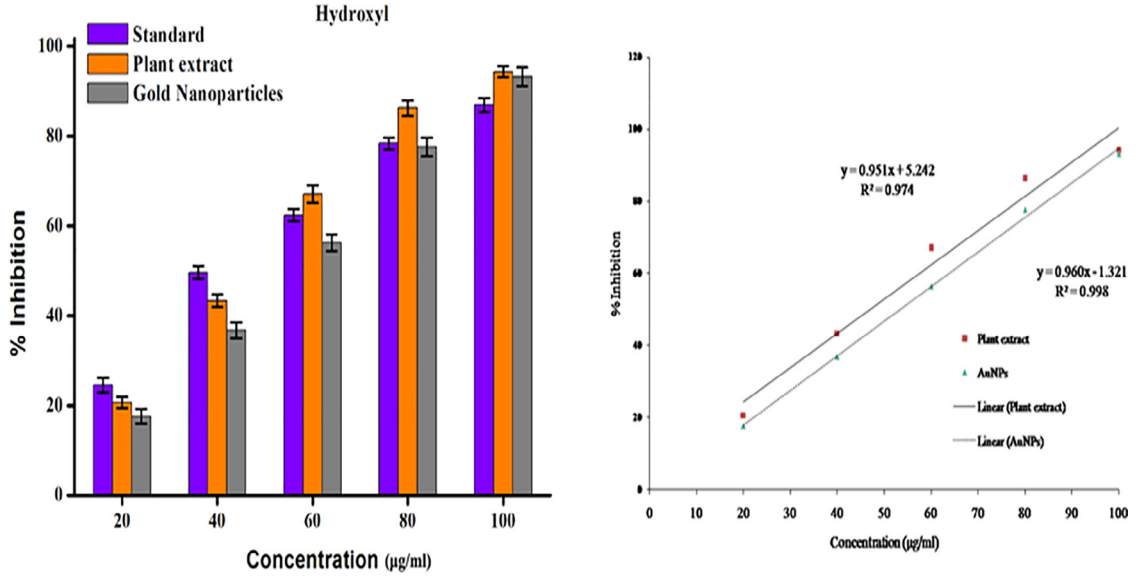

Figure S9. Antioxidant activity of gold nanoparticles and *Chamaecostus cuspidatus* plant extract by hydroxyl radical assay. *AuNPs*, gold nanoparticles.

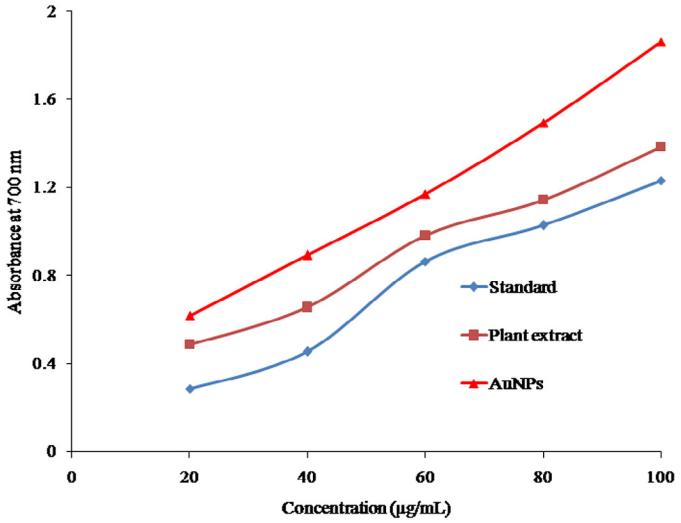

Figure S10. Effect of gold nanoparticles and *Chamaecostus cuspidatus* plant extract reducing power assay. *AuNPs*, gold nanoparticles.

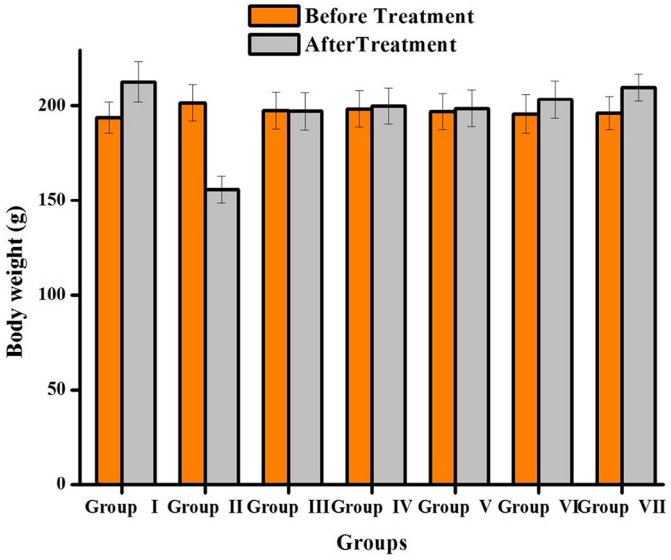

Figure S11. Effect of gold nanoparticles on changes in body weight of experimental groups.

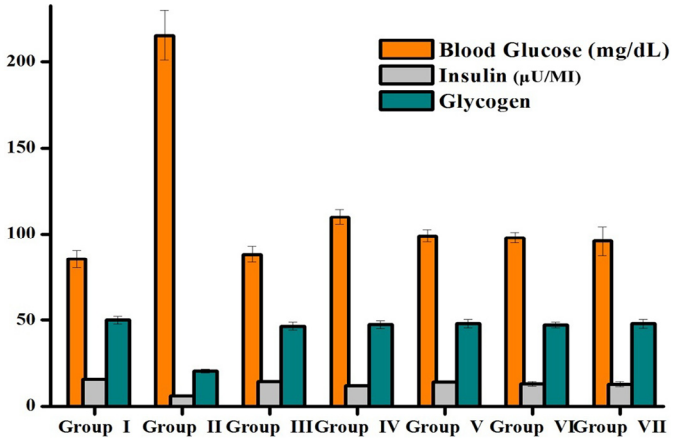

Figure S12. Effect of gold nanoparticles on changes in blood glucose, insulin and glycogen.

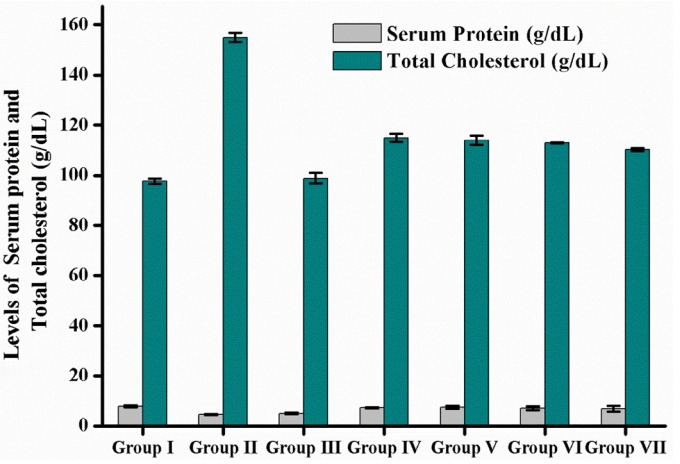

Figure S13. Effect of gold nanoparticles on changes in serum protein and total cholesterol.

Table S1
Acute toxicity study after 10 days of treatment with gold nanoparticles alone in rats

Serum number	Parameter	Control	Gold nanoparticles (1.5 mg/kg body)
1	Serum protein (g/dL)	7.77±.38	7.48±1.33
2	Total cholesterol (g/dL)	97.67±1.10	97.43±1.23
3	Blood glucose (mg/dL)	85.50±4.96	85.33±2.00
4	Insulin (µU/mL)	15.67±0.75	15.35±1.12
5	Glycogen (mg/g)	50.17±2.34	51.36±1.12

Note: Values are mean ± (n 2); statistical significance $p<0.05$ as compared with the controls.

Table S2
Effects of gold nanoparticles and aqueous extracts on changes in body weight of experimental groups of rats after 21 days of treatment

Serum number	Groups	Body weight	
		Before treatment	After treatment
1	Control	193.83±8.14	212.50±10.67
2	Diabetic	201.50±9.59	155.67±7.20
3	Standard drug (glibenclamide)	197.50±9.72	197.17±9.87
4	Diabetes + *C. cuspidatus* (300 mg/kg body weight)	198.33±9.68	199.83±9.56
5	Diabetes + *C. cuspidatus* (600 mg/kg body weight)	197.00±9.58	198.67±9.58
6	Diabetes + gold nanoparticles (0.75 mg/kg body weight)	195.8±10.18	203.4±9.65*
7	Diabetes + gold nanoparticles (1 mg/kg body weight)	196.2±8.78	209.6±7.3*

C. cuspidatus, Chamaecostus cuspidatus.
Note: Values are mean ± (n 7).
* Statistical significance $p<0.05$ as compared with the controls.

Table S3
Effects of gold nanoparticles and aqueous plant extracts on changes in blood glucose, insulin and glycogen levels

Groups	Blood glucose (mg/dL)	Insulin (μU/mL)	Glycogen (mg/g)
Control	85.50±4.96	15.67±0.75	50.17±2.34
Diabetes	215.50±14.47	6.17±0.31	20.54±1.01
Standard drug (glibenclamide)	88.33±4.61	14.38±0.71	46.50±2.17
Diabetes + *C. cuspidatus* (300 mg/kg body weight)	110.00±4.31	12.00±0.30	47.33±2.30
Diabetes + *C. cuspidatus* (600 mg/kg body weight)	99.00±3.56	14±0.20	48.00±2.44
Diabetes + gold nanoparticles (0.75 mg/kg body weight)	98.00±3.12	13±1.25	47.12±1.54
Diabetes + gold nanoparticles (1.5 mg/kg body weight)	96±8.25	12.8±1.36	47.85±2.52

C. cuspidatus, Chamaecostus cuspidatus.
Note: Values are mean ± (n 7); statistically confirmed absence of significant changes.

Table S4
Effects of gold nanoparticles and aqueous plant extracts on changes in serum protein and total cholesterol levels

Groups	Serum protein (g/dL)	Total cholesterol (g/dL)
Control	7.77±.38	97.67±1.10
Diabetes	4.7±0.20	155±1.90
Standard drug (glibenclamide)	5.06±0.33	98.83±2.13
Diabetes + *C. cuspidatus* (300 mg/kg body weight)	7.3±0.20	115±1.70
Diabetes + *C. cuspidatus* (600 mg/kg body weight)	7.4±0.60	114±1.80
Diabetes + gold nanoparticles (0.75 mg/kg body weight)	7.11±0.77	112.85±0.25*
Diabetes + gold nanoparticles (1.5 mg/kg body weight)	6.9±1.08	110.21±0.56*

C. cuspidatus, Chamaecostus cuspidatus.
Note: Values are mean ± (n 7).
* Statistical significance $p<0.05$ as compared with the controls.

Table S5
Wound areas at differing postwounding days as percentages calculated in relationship to the original wound sizes

Day	Wound healing (%)			
	Plant extract	Gold nanoparticles	Vehicle H_2O	Control
1st week	00.0±0.00	00.0±0.00	00.0±0.00	00.0±0.00
2nd week	20.5±2.05	26.5±2.65*	17.6±1.25	15.0±1.65
3rd week	42.0±2.35	64.6±2.45*	32.2±2.72	30.5±1.63
4th week	78.3±1.56	97.0±1.08*	66.6±1.15	64.9±2.45

Note: Values are mean ± (n 4).
* Statistically most significant at $p<0.01$ as compared with the controls.